EARTH SURFACE PROCESSES AND LANDFORMS
Earth Surf. Process. Landforms **43**, 3009–3021 (2018)

Published online 7 August 2018 in Wiley Online Library
(wileyonlinelibrary.com) DOI: 10.1002/esp.4464

River response to large-dam removal in a Mediterranean hydroclimatic setting: Carmel River, California, USA

Lee R. Harrison,[1]* Amy E. East,[2] Douglas P. Smith,[3] Joshua B. Logan,[2] Rosealea M. Bond,[1,4] Colin L. Nicol,[1,4] Thomas H. Williams,[1] David A. Boughton,[1] Kaitlyn Chow[3] and Lauren Luna[3]
[1] NOAA, Southwest Fisheries Science Center, Santa Cruz, CA USA
[2] US Geological Survey, Pacific Coastal and Marine Science Center, Santa Cruz, CA USA
[3] School of Natural Sciences, California State University Monterey Bay, Seaside, CA USA
[4] Institute of Marine Sciences, University of California, Santa Cruz, CA USA

Received 5 March 2018; Revised 13 June 2018; Accepted 20 June 2018

*Correspondence to: Lee R. Harrison, NOAA, Southwest Fisheries Science Center, Santa Cruz, CA 95060, USA. E-mail: lee.harrison@noaa.gov

ESPL
Earth Surface Processes and Landforms

ABSTRACT: Dam removal provides a valuable opportunity to measure the fluvial response to changes in both sediment supply and the processes that shape channel morphology. We present the first study of river response to the removal of a large (32-m-high) dam in a Mediterranean hydroclimatic setting, on the Carmel River, coastal California, USA. This before-after/control-impact study measured changes in channel topography, grain size, and salmonid spawning habitat throughout dam removal and subsequent major floods. During dam removal, the river course was re-routed in order to leave most of the impounded sediment sequestered in the former reservoir and thus prevent major channel and floodplain aggradation downstream. However, a substantial sediment pulse occurred in response to base-level fall, knickpoint migration, and channel avulsion through sediment in the former reservoir above the newly re-routed channel. The sediment pulse advanced ~3.5 km in the first wet season after dam removal, resulting in decreased riverbed grain size downstream of the dam site. In the second wet season after dam removal, high flows (including a 30-year flood and two 10-year floods) transported sediment > 30 km downstream, filling pools and reducing cross-channel relief. Deposition of gravel in the second wet season after dam removal enhanced salmonid spawning habitat downstream of the dam site. We infer that in dam removals where most reservoir sediment remains impounded and where high flows follow soon after dam removal, flow sequencing becomes a more important driver of geomorphic and fish-habitat change than the dam removal alone. © 2018 John Wiley & Sons, Ltd.

KEYWORDS: fluvial geomorphology; dam removal; channel evolution; river sediment; floods; fish habitat

Introduction

Landscape response to disturbance is one of the longest-standing problems in studies of geomorphic processes (Gilbert, 1917). Understanding how fluvial systems evolve in response to sediment-supply disturbances is critically important to assessing anthropogenic effects on watersheds (Syvitski *et al.*, 2005; Pizzuto and O'Neal, 2009; Rollet *et al.*, 2014; Yang and Lu, 2014; Reusser *et al.*, 2015), as well as to predicting river response to natural disasters (Guthrie *et al.*, 2012; Pierson and Major, 2014). However, quantifying the response to sediment-supply changes at the field scale is difficult because most substantial disturbances (e.g. landslides, volcanic eruptions) are unanticipated and rarely allow for before-after/control-impact (BACI) studies. The intentional removal of a large dam provides a rare opportunity to measure fluvial adjustment before, during, and after substantial sediment-supply and local base-level perturbations that trigger geomorphic adjustment upstream and downstream of the dam site (Pizzuto, 2002; Magilligan *et al.*, 2016; Major *et al.*, 2017).

Dam emplacement and river regulation have profound effects on river morphology and riparian ecosystems. These effects include the trapping of sediment, nutrients, and carbon in reservoirs, incision and coarsening of river channels by sediment-starved flow downstream of dams, and numerous ecological consequences of disconnecting upstream and downstream river ecosystems (Galay, 1983; Ward and Stanford, 1995; Poff and Hart, 2002; Grant *et al.*, 2003; Schmidt and Wilcock, 2008; Kondolf *et al.*, 2014). Dam removal is becoming more common as a means to effect at least partial geomorphic and ecosystem restoration in anthropogenically altered watersheds (Bednarek, 2001; Doyle *et al.*, 2008; Pess *et al.*, 2014; Magilligan *et al.*, 2016; Foley *et al.*, 2017a), as well as to remove economic liability associated with aging or unsafe dams. Few large dams (> 10 m tall) have been removed thus far, however, and comprehensive studies of fluvial response to dam removal (especially large dams) are not only rare in the scientific literature, but also represent a limited biogeographic scope (Bellmore *et al.*, 2017; Foley *et al.*, 2017b; Major *et al.*, 2017). Few studies have investigated dam removals in

Mediterranean hydroclimates, where historical impacts of dams are large and fluvial evolution tends to be dominated by distinctive episodic flow and sediment regimes not found elsewhere.

Existing studies of sedimentary and geomorphic response to dam removal indicate that rates of geomorphic change and sediment export can decline fairly rapidly (within 1–2 years) following the disturbance caused by reservoir-sediment erosion and transport during and after dam removal (Warrick *et al.*, 2015; Foley *et al.*, 2017a). Geomorphic adjustment upstream of a former dam site commonly includes knickpoint migration and channel incision through the reservoir sediment deposit (Doyle *et al.*, 2003; Wildman and MacBroom, 2005; Major *et al.*, 2012; Bountry *et al.*, 2013; Randle *et al.*, 2015; Wang and Kuo, 2016). The introduction of sediment pulses to river channels commonly results in bed aggradation as the introduced sediment pulse translates downstream as a discrete wave, disperses in place or evolves through a combination of translation and dispersion (Lisle *et al.*, 2001; Cui *et al.*, 2003a; Sklar *et al.*, 2009). New sediment deposition below the dam site fills pools in the channel bed, and can form new bars that increase both channel braiding and the transfer of water from the channel to the floodplain; new deposition also commonly decreases the riverbed grain size (Pearson *et al.*, 2011; Major *et al.*, 2012; Evans and Wilcox, 2014; Tullos *et al.*, 2014; Wilcox *et al.*, 2014; East *et al.*, 2015; Zunka *et al.*, 2015; Collins *et al.*, 2017). These effects wane over time as the sediment pulse migrates downstream and the flow incises through the new deposits (East *et al.*, 2015), but reconnection with upstream sediment supply is anticipated to transport additional sediment to the downstream river over the long term.

We used a BACI study design to evaluate the river response to removal of 32-m-high San Clemente Dam on the Carmel River, central California coast. This was the third-tallest dam removed intentionally thus far globally (Major *et al.*, 2017), and provided a case study that is unusual in three respects. First, as the largest dam removal in a Mediterranean hydroclimatic setting (Ibisate *et al.*, 2016), the potential for transporting sediment and restructuring channel morphology differed from previous large-dam-removal situations. As is typical for Mediterranean-type rivers, the Carmel River flow varies over more than three orders of magnitude seasonally; all of its sediment-transport capacity occurs during a winter rainy season, with no secondary contribution from spring snowmelt high flows. The ecosystem composition thus also differed from that in previous studies of large dam removals, which have focused on US Pacific Northwest biotic communities (Tonra *et al.*, 2015; Allen *et al.*, 2016; Claeson and Coffin, 2016; Quinn *et al.*, 2017). Second, whereas most dam removals release stored reservoir sediment by natural river erosion, the majority of sediment impounded by San Clemente Dam remained sequestered by design after dam removal. The Carmel River was re-routed to bypass the downstream two-thirds of the reservoir sediment deposit (details later). Finally, whereas the first wet season after dam removal exhibited drier than normal conditions, the second wet season was one of the wettest on record for this watershed, providing a natural experiment on the interaction of dam removal with the episodic flow regime characteristic of Mediterranean hydroclimatic settings. Measuring the effects of floods in that second wet season allowed us to re-evaluate a tentative conclusion of previous dam-removal synthesis studies – that flow sequencing tends to be a less-important driver of geomorphic response than is the degree of base-level fall or released sediment volume (Grant and Lewis, 2015; Foley *et al.*, 2017a; Major *et al.*, 2017).

In this study we demonstrate that when a substantial proportion of reservoir sediment remains impounded — as will likely be the case in many future dam removals where contaminated sediment is a concern, or where downstream aggradation must be minimized to protect infrastructure (Evans and Wilcox, 2014; Claeson and Coffin, 2016) — high flows can be relatively more important as drivers of channel change than is the dam removal alone. We show that high flows early in the dam-removal response time frame can substantially affect fluvial evolution in the newly exposed reservoir sediment, promoting new channel avulsion rather than the incision and lateral meander migration that dominated other recent examples of fluvial processes in newly exposed reservoir deposits. We characterize geomorphic and sedimentary responses in terms of alteration from the dammed condition, and assess the potential of the post-dam-removal channel for enhancing salmonid substrate habitat quality and quantity.

Study Area

The Carmel River drains ~650 km^2 of steep terrain (maximum elevation 1540 m) in the Santa Lucia Mountains of central California, entering the Pacific Ocean just south of Monterey Bay (Figure 1). Most of the watershed draining into the study area is composed of steep slopes of fractured, highly weathered granitic substrate and talus, overlain by chaparral vegetation (Smith *et al.*, 2004). The lowermost ~40 km of the Carmel River alternates between bedrock and alluvial morphology; most of the mainstem channel can be characterized as a single-thread gravel-bed river with a fairly straight planform (mean sinuosity = 1.17). Sediment supply to the upper river is dominated by landslides and dry ravel. Human land use in the basin includes rural communities and agriculture, but much of the upper basin remains undeveloped. The landscape is episodically modified by wildfire, and parts of the upper watershed burned during the study period (2015 and 2016). The greatest burn intensity was in the upper watershed above Los Padres Dam (Figure 1a), which traps sediment from 18% of the Carmel watershed upstream of our study reaches. While our visual observations suggested that tributary sediment yield downstream of Los Padres Dam may have increased thereafter, wildfires in these regions caused little vegetation loss along the mainstem river corridor and we observed little apparent fire influence on sediment yield near our study sites.

Hydrology of the Carmel River is driven by the intensity and location of landfall of weather systems in the northern Pacific Ocean. Rainfall occurs predominately during a winter wet season (November–March), either from storms originating in the Gulf of Alaska or from warm Central Pacific 'atmospheric river' systems. Atmospheric-river storms cause intense rainfall, and commonly flooding, in the mountains of coastal California (Dettinger, 2011). Although wet years, and thus greater sediment export, are generally associated with the El Niño phase of the El Niño–Southern Oscillation (ENSO) cycle (Cayan *et al.*, 1999; Andrews and Antweiler, 2012; Gray *et al.*, 2015), some of the largest regional floods have occurred during ENSO-neutral years, which are thought to facilitate the transport of atmospheric-river water vapor toward the California coast (Bao *et al.*, 2006). The winter of 2017 (the final year of this study, a La Niña year) had multiple floods induced by atmospheric-river precipitation, including four ~two-year floods, two 10-year floods, and one 30-year flood event (Figure 2a). These flood flows brought peak discharge more than two orders of magnitude above the Carmel River's mean annual flow (2.6 m^3/s) and more than three orders of magnitude above its summer low flows (~0.1 m^3/s).

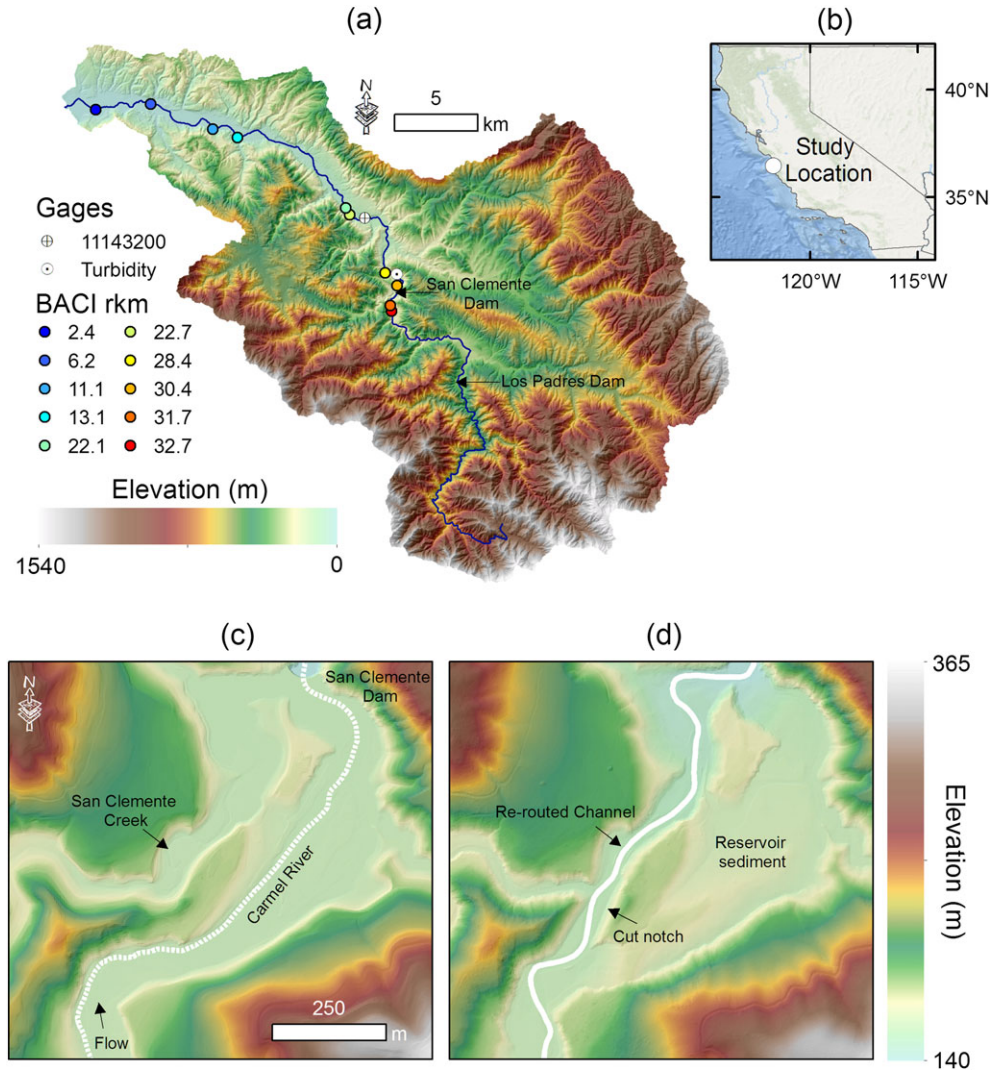

Figure 1. Field setting on the Carmel River, California including (a) Carmel River watershed elevation map and field sites, where each before-after/control-impact (BACI) site is colored by the river kilometer (rkm) from the Pacific Ocean. (b) California inset map. Digital elevation models of the Carmel River (c) before and (d) after removal of San Clemente Dam. The former position of San Clemente Dam is shown in (a) and (c) for reference. [Colour figure can be viewed at wileyonlinelibrary.com]

The 32-m-tall San Clemente Dam was constructed at river-kilometer (rkm) 30.5 in the early 1920s as a water-resource project to support regional development. The 40-m-high Los Padres Dam was built in the 1940s, ~11 km upstream at rkm 42. San Clemente Dam was removed in November 2015 after having been found structurally unsound. By that time the reservoir had lost 95% of its original capacity and was filled almost completely with ~1.7 million m^3 of sediment (MEI, 2005), providing little water-storage capacity. The reservoir deposits had a median sediment diameter (D_{50}) of 0.57 mm, with 85.5% of the reservoir material being classified as sand or finer and 14.5% as gravel (MEI, 2005). To prevent downstream aggradation that could have increased the flood risk to structures on the floodplain, most of the sediment was permanently sequestered in the reservoir area. This was achieved coincidently with dam removal by cutting a new channel through a bedrock ridge that formerly separated the Carmel River from a nearby tributary, San Clemente Creek, and re-

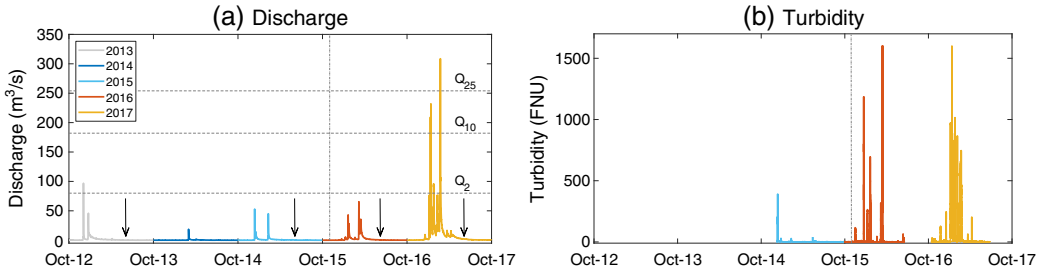

Figure 2. (a) Carmel River hydrograph at the USGS gage #11143200, with individual water years (2013–2017) represented as uniquely colored lines. The horizontal dashed lines denote the magnitude of the 2, 10 and 25-year flood events, based on Log-Pearson Type-III analyses, using peak flow data from 1956 to 2017. Vertical arrows indicate the general timing of before-after/control-impact (BACI) field campaigns. (b) Turbidity time series with turbidity values shown in formazin nephelometric units (FNU). [Colour figure can be viewed at wileyonlinelibrary.com]

routing the mainstem river through the newly breached ridge to join San Clemente Creek 700 m upstream of the natural confluence and approximately one-third of the longitudinal distance through the reservoir deposit (Figures 1c and 1d). Thus, only the upstream third of the reservoir sediment underwent base-level fall and subsequent erosion during and after dam removal.

The aquatic ecosystem of the Carmel River hosts *Oncorhynchus mykiss*; the anadromous form (steelhead) of this fish are listed as threatened under the US Endangered Species Act. Steelhead require clean gravel substrates for spawning and deep pools for rearing, and one of the goals of dam removal was to improve steelhead habitat conditions. San Clemente Dam did not entirely block fish migration, but the steepness of a fish ladder formerly in place along one side of the dam (the steepest fish ladder on the US west coast) limited upstream passage for adults and upstream–downstream passage for juvenile steelhead. Although not a complete watershed restoration (Los Padres Dam remains in place), removal of San Clemente Dam was anticipated to induce physical changes that would enhance habitat and passage for various life stages of steelhead (Boughton *et al.*, 2016).

Methods

We quantified the geomorphic and steelhead habitat response to dam removal in 10 reaches using a BACI study design. Study reaches included one control site and nine impact sites (see Table I for reach attributes). The control site, immediately upstream of the San Clemente reservoir, was unaffected by any activity related to San Clemente Dam removal. The goals of using the control site were to document whether there was substantial sediment being delivered from hillslopes and tributaries upstream of the dam removal site and to provide a baseline from which to compare the post-dam removal response at the impact sites. The impact reaches included one in the upstream portion of the former reservoir, above the re-route channel, one immediately below the former dam site and seven additional reaches in the ~30 km between the dam site and the river outlet (Figure 1 and Table I).

At each site we conducted annual surveys of topography and bed-sediment grain size for two years before (2013, 2015) and two years after (2016, 2017) dam removal. We used aerial photography to map planform changes in the reservoir reach before and after dam removal. Sediment delivery below the former dam site was monitored using turbidity measurements (Figure 2b). We related changes in sediment texture to steelhead spawning habitat suitability pre- and post-dam removal.

Turbidity and suspended sediment

To quantify the timing and magnitude of sediment transport, continuous turbidity data were collected at 15-minute intervals using a DTS-12 sensor from December 2014 through July 2017 (Figure 2b). The DTS-12 sensor had a calibrated upper limit of 1600 FNU (formazin nephelometric units). The sensor was installed adjacent to a long-term stream gage managed by the Monterey Peninsula Water Management District (MPWMD), located 1.3 km downstream from the dam removal site (rkm 29.2). Discrete depth-integrated suspended-sediment samples were also collected over a range of streamflow conditions using a DH-48 sampler from a bridge 50 m downstream of the DTS-12 sensor. Cross-sectional suspended-sediment samples were collected in equally spaced increments across the width of the channel and were analyzed for suspended-sediment concentrations (SSC). Data were collected and analyzed using US Geological Survey (USGS) protocols (Guy, 1969; Rasmussen *et al.*, 2009).

The depth-integrated samples were used to develop a regression model between turbidity and SSC, in order to estimate 15-minute SSC values. Uncertainty in the suspended sediment rating curve was estimated by generating the 95% confidence interval (c.i.) using Monte Carlo simulations. The values bounding 95% of the simulated values are reported in the results. Calculations of suspended-sediment load were made for the year prior to dam removal, and the first two years after the dam was removed. Computed suspended-sediment flux was estimated as the product of sediment concentration (in mg/L) and discharge (in m^3/s) and reported in tonnes. Our sediment delivery estimates have low accuracy because the rating lacks samples from high flow events, and they likely underpredict the total sediment flux because there were no bedload measurements.

Reservoir planform change analysis

We mapped planform changes in the reservoir reach using three sets of aerial photographs acquired before (2015) and after (2016, 2017) dam removal. For each photograph, we digitized channel banks and interpolated a centerline as the midpoint between banklines. The river migration distance was measured by fitting Bezier curves between the older and newer interpolated centerlines (Lauer and Parker, 2008), with migration distances calculated in 5-m increments along the 850-m reach. We estimated the sediment volume eroded from the upper reservoir reach in 2016 and 2017 as the product of the lateral migration distance, mean outer bank height and reach length. We converted sediment volume estimates to mass

Table I. Physical characteristics of the before-after/control-impact (BACI) study reaches on the Carmel River, California

Reach	River kilometer	Average gradient (m/m)	Average bankfull width (m)	Average valley width (m)	Confinement (m/m)	Initial D_{50} (mm)
Control	32.7	0.0033	20.8	68	3.3	39.0
Reservoir	31.7	0.0024	20.9	111	5.3	13.9
San Clemente Dam	30.4	0.0138	22.4	39	1.8	149.7
Sleepy Hollow	28.4	0.0085	14.7	76	5.2	94.9
Upper DeDampierre	22.7	0.0035	17.9	261	14.6	59.0
Lower DeDampierre	22.1	0.0021	20.4	197	9.7	45.3
Berwick	13.1	0.0021	8.7	82	9.4	38.8
Schulte Road	11.1	0.0020	15.9	135	8.5	23.4
San Carlos	6.2	0.0019	16.0	320	20.0	15.3
Crossroads	2.4	0.0018	14.0	845	60.2	16.9

(in tonnes) in order to facilitate comparison with sediment loads estimated from the below-dam sediment rating curve. We used a range of bulk density values between 1200 and 1900 kg/m^3 for the coarse upper Carmel reservoir sediment (sand and coarser), based on bulk density values in comparable reservoir sediments from Lake Aldwell and Lake Mills on the Elwha River reported by Warrick *et al*. (2015). The use of aerial photographs to investigate lateral channel changes and sediment storage change was only possible in the reservoir reach due to the dense riparian canopy, which obscured most of the wetted river channel in the other nine reaches.

Quantifying geomorphic change

In each of the 10 reaches, we surveyed six cross-sections during summer low-flow conditions. We established a network of control points using real-time kinematic (RTK) global positioning system (GPS) units and then used a combination of total-station and auto-level surveys to measure topography along cross-sections oriented perpendicular to the channel. Cross-sections were spaced approximately 50 m apart, with a typical cross-stream point spacing of 1 to 2 m; points were spaced more densely along breaks in slope and in areas of more complex topography.

We used the cross-sectional survey data from each reach to investigate longitudinal changes in the sediment thickness and cross-stream relief over time. Following Zunka *et al*. (2015), we defined the cross-channel bed relief (r) as the difference between the deepest part of a cross-section and the highest feature within the bankfull channel. The mean sediment thickness at a cross-section (z) was calculated as $z = A/B$, where A equals the cross-sectional area across the bankfull channel width (B) for each survey year (Zunka *et al*., 2015). The same width (B) was used for each survey year for a given cross-section.

We anticipated increased sediment deposition in large pools following dam removal and conducted high-resolution surveys in two large pools located at rkm 30.4 and 28.4 in 2015–2017. Bed elevations were measured using high-precision total stations (1–2 cm vertical and horizontal uncertainty). In areas too deep to wade, a survey prism was mounted on an inflatable kayak and configured to measure water surface elevations using a robotic total-station, while a Sonarmite echo sounder (reported accuracy = 1 cm) recorded water depths. The topographic surveys had a mean point density of 1.3 pts/m^2. Each data set was interpolated to form a continuous surface using Delaunay triangulation and then resampled onto a digital elevation model (DEM) with 0.3 m resolution.

We assumed uncertainty in the DEMs was mainly due to interpolation, as the instrument error in our surveys was on the order of 1 to 2 cm. Interpolation error was estimated using a bootstrap test, randomly separating 10% of the survey data as check points and performing a grid-to-point comparison (Brasington *et al*., 2012). This analysis found that the standard deviation of absolute errors (the difference between surveyed elevation and DEM elevation) ranged from 0.070 to 0.1 m. We generated DEMs of difference (DoDs) for each site by subtracting each successive DEM using the approach of Wheaton *et al*. (2010). We assigned spatially uniform uncertainty of 0.12 m to each surface based on our estimates of the instrument error and interpolation errors associated with converting the point data to a continuous DEM. The uncertainty in the DoD was approximated using the probabilistic thresholding approach of Lane *et al*. (2003) set at the 95% c.i.

Sediment grain size

Distributions of bed-sediment grain size were obtained in each of the 10 study reaches, using the Wolman pebble-count method (Wolman, 1954). Grains were measured within the bankfull channel along the same transects where we surveyed channel topography. We divided the bankfull width into quantiles and collected 20 grain size measurements at each quantile using a 0.5 m × 0.5 m sampling frame and grain size template, generating 100 or more grain sizes per transect.

Spawning-habitat predictions

Salmonid fish such as *O. mykiss* require riverbed sediment within a certain range of grain-sizes to facilitate spawning (Kondolf and Wolman, 1993). The grain size must be fine enough for the fish to be able to move particles while excavating a redd (i.e. egg nest), but coarse and well-sorted enough for water to flow through pore spaces, maintaining oxygen supply to the eggs. To investigate how the quantity and quality of spawning habitat adjusted after dam removal, we predicted the spawning substrate suitability using grain-size distributions generated from the pebble counts. We calculated a dimensionless index of substrate suitability using habitat suitability curves previously developed for adult steelhead in the Carmel River (Dettman and Hanna, 1991). The spawning substrate habitat suitability curve indicated that high-quality spawning-habitat on the Carmel River (indicated by a suitability index value $>$ 0.7) ranged from roughly 30 to 55 mm (Dettman and Hanna, 1991). Spawning-habitat suitability also varies with water depth and velocity; however, accounting for changes in flow hydraulics would have required the development of hydrodynamic models, which was beyond the scope of this study. Nevertheless, our field observations indicated little appreciable change in the topography or hydraulics of riffles frequently used for spawning, therefore our approach of focusing solely on the changes in substrate size and texture should provide a first-order approximation of available spawning habitat conditions.

Results

To evaluate the sedimentary and geomorphic changes in the Carmel River between 2013 and 2017, we considered both the dam-removal events and timeline as well as the concurrent hydrology. Later, we summarize the hydrologic conditions over those four years as well as the results of our sedimentary and geomorphic measurements, and attempt to distinguish the relative importance of each driver of change.

Turbidity and sediment load

In the water year immediately prior to dam removal (2015), there were two modest flow peaks with return intervals of $<$ two-years (Figure 2a). The first produced a single spike in the turbidity record, with a peak value of ~400 FNU (Figure 2b). The water year during and after dam removal (2016) had two more flow events of similar magnitude (Figure 2a), which caused multiple turbidity spikes, with peak values $>$ 1600 FNU (Figure 2b), the calibrated upper limit of the DTS-12 sensor. In the second year after dam removal (2017) a series of flood events were associated with multiple large increases in turbidity (Figure 2b).

Based on the suspended-sediment rating curves, we estimated that 230 ± 100 tonnes of sediment (95% c.i.) were

delivered to the below-dam reach in the year prior to dam removal. In the first year after dam removal, sediment delivery to downstream reaches increased about 10-fold, with estimated sediment mass fluxes of 2550 ± 1050 tonnes (95% c.i.). The peak flows in the second year after dam removal produced an additional ~20-fold increase in sediment delivery, with sediment mass flux of 49 000 ± 21 000 tonnes (95% c.i.).

The dynamic relation between discharge and turbidity demonstrated consistent evidence for sediment-supply limited conditions for each of the 2017 floods (Figure 3). The term sediment-supply limited is used here to indicate that the flow transport capacity exceeded the sediment supply over the duration of an individual flood (Topping *et al.*, 2000). Clockwise hysteresis between water discharge and turbidity is clearly evident in each of the flood events, with greater turbidity values on the rising limb of the hydrograph than on the falling limb (lower panels in Figure 3). This shows that although each flood increased turbidity values, the transport capacity appeared to outpace the sediment supply over the course of each flood. This pattern likely indicates a lack of sediment delivery late in the floods from the upper watershed, indicative of overall sediment supply-limited conditions (Klein, 1984; Topping *et al.*, 2007; Conaway *et al.*, 2013). The sediment supply also appeared to diminish throughout the water year, with lower peak turbidity values in the latest and largest flood (Figure 3h) compared to the earlier floods (Figures 3b, 3d and 3f); this is consistent with a generally sediment-supply limited system.

Reservoir channel evolution

The degree of reservoir planform changes varied in response to the sequencing of post-dam-removal floods (Figure 4). Mean distances of lateral channel migration were small (~1 m) in the upper reservoir reach in the first year after dam removal (Figure 4b). In the second year after dam removal, the channel migrated by up to 45 m, with a mean lateral shifting rate of 19 m (Figure 4c). The 2017 floods caused substantial geomorphic change including river channel widening, avulsion of a new channel through the upper part of the reservoir deposit and extensive meander bend migration (Figure 4c). Planform changes in the upper reservoir reach resulted in eroded sediment volumes of 2125 and 48 450 m^3 and eroded masses of 2000 ± 450 (tonnes) and 45 050 ± 10 175 (tonnes) in the first and second year after dam removal, respectively. Uncertainty in the sediment mass estimates stems from our usage of a range of bulk density values between 1200 and 1900 kg/m^3 after Warrick *et al.* (2015). Reservoir sediment mass values represent 78 and 92% of the total sediment masses recorded by the below-dam turbidity sensor in the first and second year following dam removal.

Longitudinal changes in sediment thickness and relief

We measured little change in the mean, longitudinal thickness of sediment (z) prior to dam removal (Figure 5a). Upstream of the dam site, the control reach showed virtually no change in sediment thickness over time (rkm 32.7; Figures 5a–5c). The two small flow events that occurred in the first year after dam removal (WY 2016) caused net incision of −0.24 m in the reservoir reach (rkm 32), and net deposition of 0.15 m in the rkm 28.4 reach below the dam (Figure 5b). The deposition patterns in the reaches below the dam site indicated the presence of a sediment pulse, with the leading edge terminating ~3.5 km below the former dam site as of spring 2016 (rkm 27; Figure 5b). The series of large flood events in 2017 which accelerated reservoir erosion led to a second sediment pulse, with deposition occurring at least 25 km downstream from the former dam site (rkm 6; Figure 5c). Our field observations suggest that the sediment pulse in fact traveled > 30 km and reached the Pacific Ocean, as new sand deposits were observed near the river outlet after the 2017 flood events. While it is possible that a portion of the sediment pulse may have been introduced by tributaries located downstream from the dam, we did not observe clear

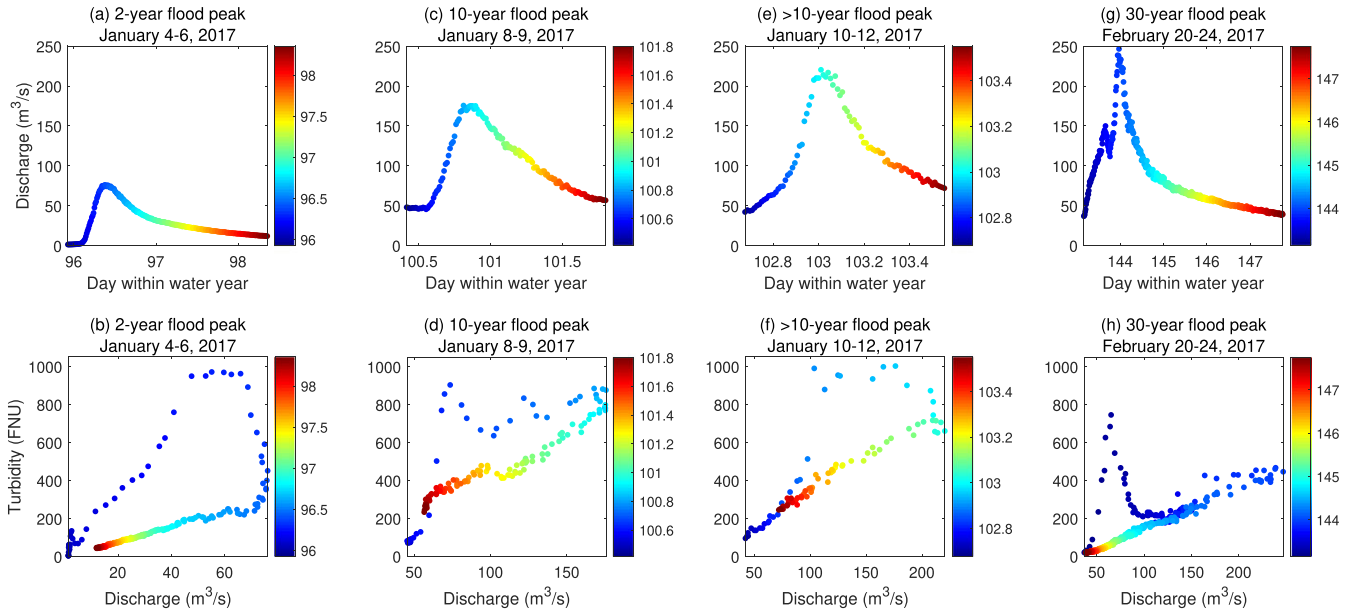

Figure 3. Relation between discharge (upper panels) and turbidity (lower panels) for four flood events during the 2017 water year, where each point is color-coded by time. Clockwise hysteresis between discharge and turbidity is evident in all floods (lower panels). Note the discharge values on the *x*-axis (lower panels) vary to show more detail in the hysteresis loops. [Colour figure can be viewed at wileyonlinelibrary.com]

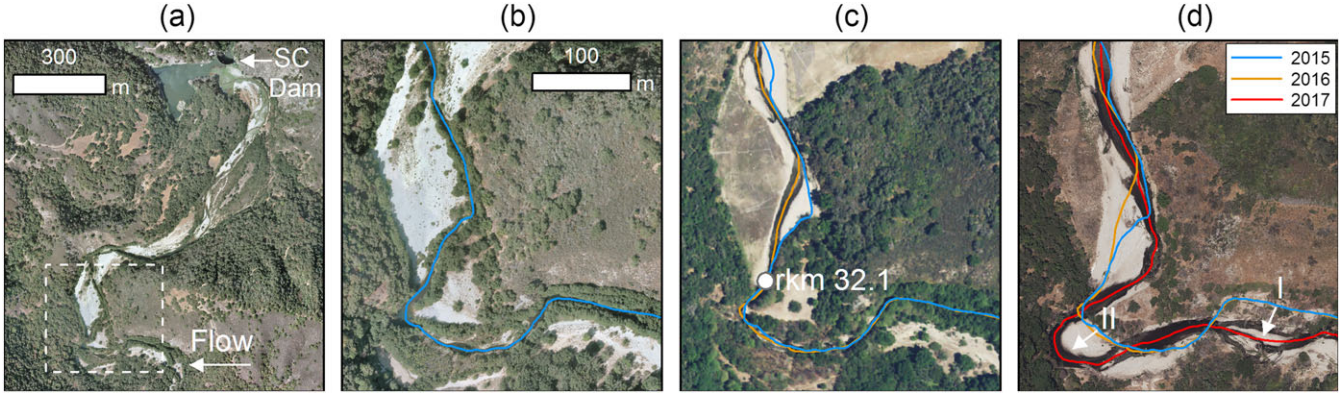

Figure 4. Planform changes in the upper San Clemente Reservoir. (a) Aerial photograph of the pre-dam removal reservoir, where the white box indicates the location of (b) to (d). (b) 2015 aerial photograph and digitized river centerline (blue) illustrating the pre-dam removal channel configuration. (c) Construction activities downstream of rkm 32.1 involved channel straightening and vegetation removal, while upstream changes included ~1 m of lateral shifting in the first year following dam removal. (d) Large floods in 2017 generated channel avulsion (I) and increased meander migration (II). [Colour figure can be viewed at wileyonlinelibrary.com]

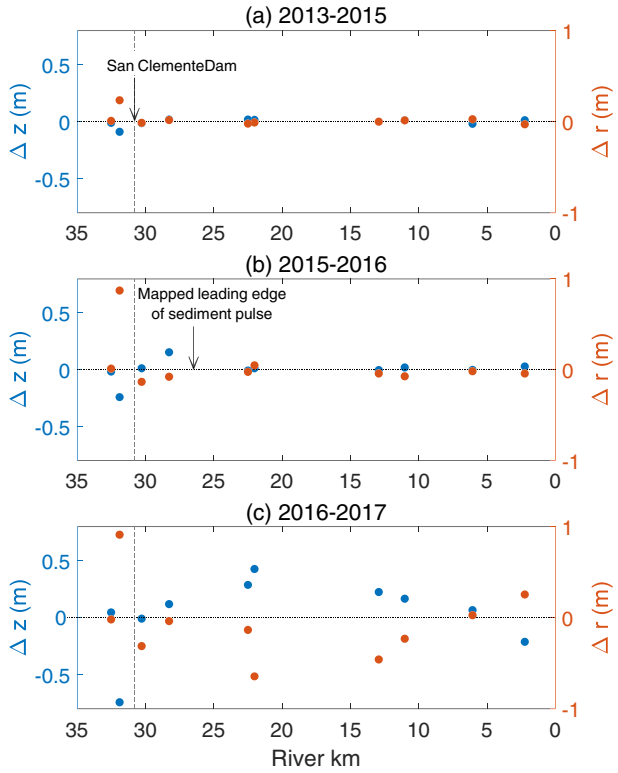

Figure 5. Downstream changes in the net sediment thickness, Δz (blue circles) and relief, Δr (orange circles), where individual data points represent reach-averaged values. Horizontal dotted lines indicate zero change and the vertical dashed line marks the location of the former San Clemente Dam. [Colour figure can be viewed at wileyonlinelibrary.com]

indicators of increased sediment supply from tributaries during or after storm events, such as turbid water or alluvial fans located at tributary junctions. Thus we interpret the upstream reservoir sediment as the primary source of the sediment pulse.

Vertical incision within the reservoir reach consistently increased cross-channel relief (r), while sediment deposition below the dam decreased relief at the majority of downstream sites (Figures 5b and 5c). The largest decreases in relief occurred in lower-gradient reaches near rkm 22, in an area where the valley width increases and the slope abruptly diminishes (Figure 5c). The finer-grained, downstream-most reach experienced net lowering and a slight increase in cross-channel relief.

Reach-scale morphologic adjustments

Topographic surveys found substantial reach-scale, geomorphic changes in the reservoir and below dam reaches over time (Figure 6). The reservoir reach underwent extensive bank erosion, vertical incision and knickpoint retreat, which originated during pre-dam removal construction activities (2015) and continued in the two years following dam removal (Figure 6b). Downstream of the dam removal site, the primary geomorphic response was sediment deposition in pools and runs, with minimal to no bed-elevation changes in riffles (Figures 6c–6f). The sites at rkm 30.4 and rkm 28.4 (the two closest to the former dam) experienced decimeters of deposition in pools in 2016 (Figures 6c and 6d), with minimal overbank deposition. Study reaches farther downstream experienced a combination of pool filling and overbank deposition (Figures 6e and 6f) in response to the high flows in winter 2017. The control reach remained virtually unchanged over time (Figure 6a), indicating that dam removal was primarily responsible for the observed geomorphic adjustments.

Detailed pool surveys illustrated the overall pattern of pool filling and gradual evacuation of sediment (Figure 7). In the downstream pool closest to the dam removal site (rkm 30.4), the total net volumetric change was 306 ± 107 m^3 of sediment deposited in the first year after dam removal, resulting in a mean net sediment thickness change of 0.37 m and maximum deposition of 1.3 m in the deepest portion of the pool (Figure 7a). Deposition was focused mainly in the central region of the pool, with more subtle deposition along the channel margins. The high flows in 2017 generated a net loss of −822 ± 125 m^3 of sediment, with mean sediment thickness change of −0.93 m and maximum erosion of −1.9 m (Figure 7b). These results indicate that the initial sediment deposit was flushed out completely during winter 2017 and the pool volume actually increased by roughly 50% (~515 m^3) relative to the pre-dam removal channel.

The deep pool in the reach surrounding rkm 28.4 experienced a net volumetric change of 844 ± 110 m^3 in the first year after dam removal, with a mean net sediment thickness change of 0.91 m and maximum deposition of 3 m (Figure 7c). Sediment storage was concentrated on the point bar along the inner bank and in the central portion of the pool (Figure 7c). High flows in 2017 produced a combination of scour and fill at this site, with 61% of the pool area experiencing erosion and 39% experiencing deposition (Figure 7d). A total of −264 ± 87 m^3 of sediment was eroded from the pool, mainly at the pool head. The floods deposited 169 ± 44 m^3 of sediment along both

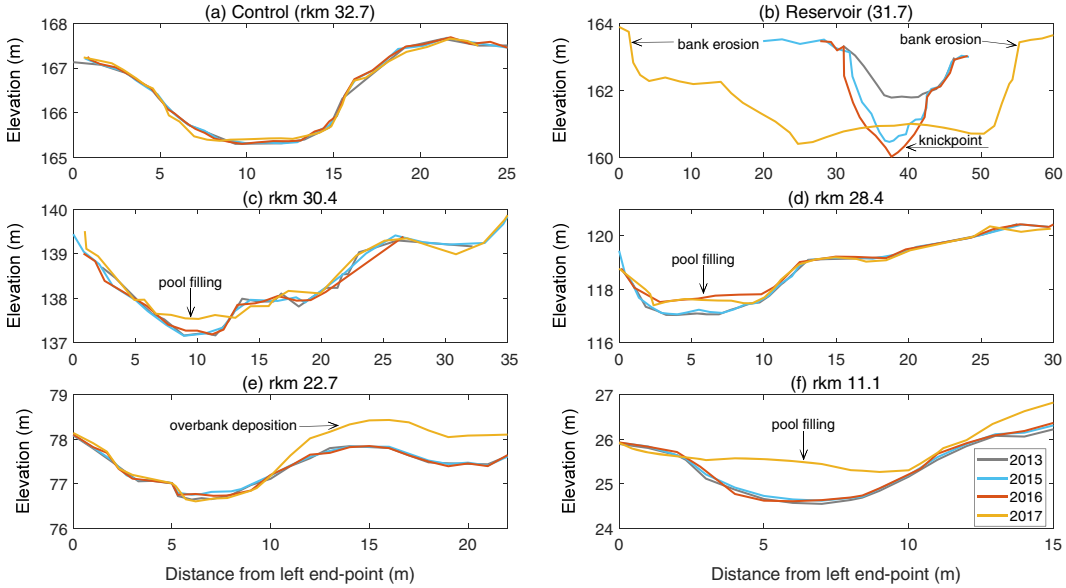

Figure 6. Illustrations of the general morphologic responses at example cross-sections from the (a) control, (b) reservoir and (c–f) below dam reaches. Reach locations are provided in Figure 1a. [Colour figure can be viewed at wileyonlinelibrary.com]

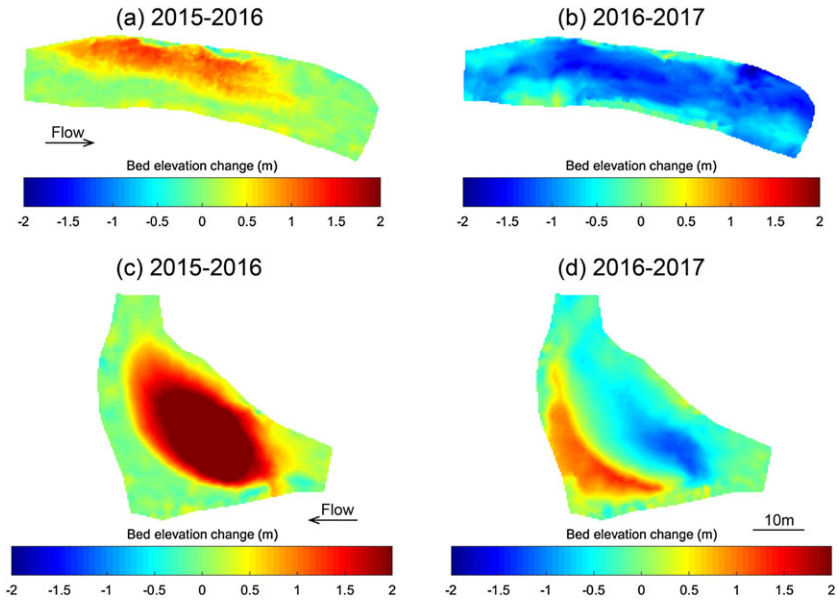

Figure 7. Digital elevation models of difference illustrating pool sedimentation dynamics in the rkm 30.4 (a,b) and 28.4 (c,d) reaches. [Colour figure can be viewed at wileyonlinelibrary.com]

banks and the pool tail (Figure 7d). Based on the net sediment storage calculations, approximately 750 m^3 of sediment introduced in 2016 remained in the pool after 2017.

Bed grain-size and spawning gravel evolution

Our measurements of bed-sediment grain size revealed changes in the longitudinal pattern of grain size through time (Figure 8). The geometric mean of sediment grain size (D_g) showed minimal change within our control reach, consistent with the morphologic response there (Figures 8a–8d). The gradual downstream fining pattern observed along many rivers was evidently disrupted by the presence of San Clemente Dam; we infer that sediment trapping behind the dam had resulted in coarse (armored) sediment in the two reaches directly below the former dam site (rkm 30.4 and 28.4; Figures 8a and 8b). Following dam removal, the introduction of sand and fine gravel decreased the D_g from 94 to 26 mm (Figure 8c) in the two reaches immediately below the former dam site. The decrease in D_g was driven largely by an influx of sand, which increased from 7% to 30% of the total proportion of measured sediment grains following dam removal in the rkm 30.4 and 28.4 reaches. The largest changes in grain size were observed in downstream pools (rkm 30.4 to 2.4), where the mean proportion of sand fractions increased from 29% before dam removal to 51% after dam removal.

Dam removal and subsequent high flows generated a modest increase in steelhead spawning substrate quality in reaches near the former dam site and a decrease in spawning substrate quality further away from the dam. In the pre-dam-removal surveys, the sites closest to the dam contained limited high-quality spawning gravel, with 5–20% of the riffle substrates categorized as high-quality spawning substrate (rkm 30.4 and 28.4; Figures 9a and 9b). In the first year after dam removal, there was a small influx of gravel to the rkm 28.4 reach, resulting in

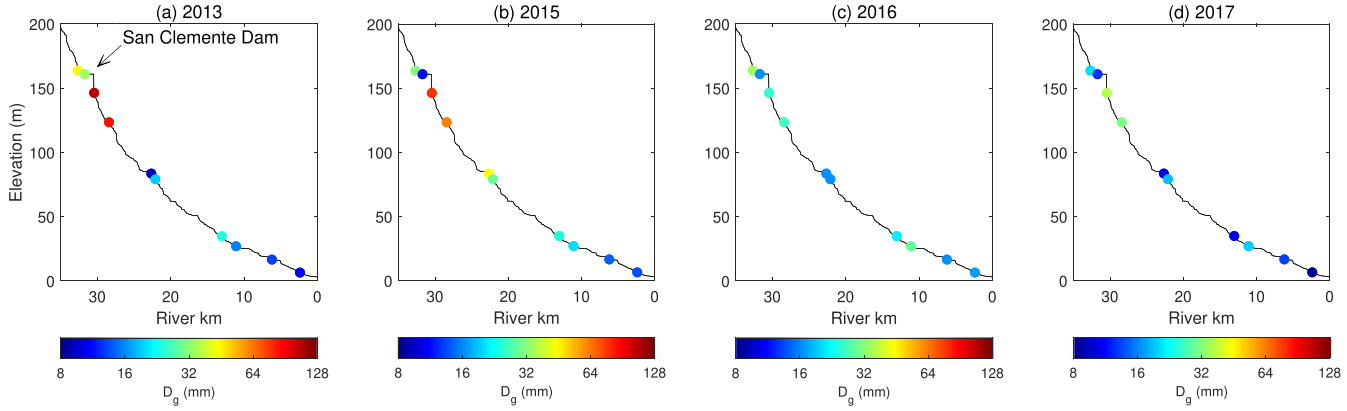

Figure 8. Longitudinal changes in geometric mean (D_g) sediment grain size through time. Individual data points represent reach-averaged values for a given year. [Colour figure can be viewed at wileyonlinelibrary.com]

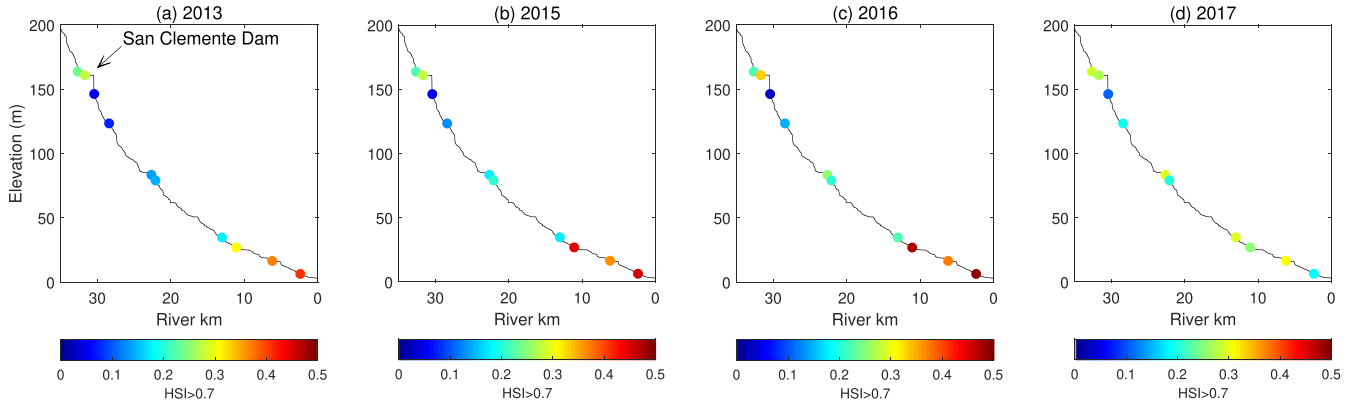

Figure 9. Fractional changes in high-quality steelhead spawning substrate through time. Data points represent the reach-averaged proportion of each pebble count with a habitat suitability index (HSI) score > 0.7. [Colour figure can be viewed at wileyonlinelibrary.com]

a modest (16%) increase in high-quality spawning substrate (Figure 9c). The floods of 2017 introduced larger volumes of finer gravel, resulting in a 50–69% increase in high-quality spawning substrate at the four sites closest to the dam (rkm 30.4 to 22.1; Figure 9d). The more distal, lower-gradient reaches initially had between 30 and 50% of the riffle area characterized by high-quality spawning substrate, but between 44 and 60% of this suitable substrate was lost in 2017, as the gravel bed was covered in sand (Figure 9d).

Discussion

After removal of San Clemente Dam, the coupled processes of reservoir-sediment erosion and downstream deposition on the Carmel River varied as a function of the post-dam-removal hydrology, in contrast to the geomorphic response measured after several other large dam removals. During the recent removal of Elwha and Glines Canyon Dams in Washington, reservoir sediment erosion largely depended on the rate of reservoir drawdown, whereas after dam removal reservoir sediment erosion was driven by flow conditions. Reservoir sediment erosion on the Elwha was greatest by far during the initial stages of dam removal (when driven by drawdown rate, i.e. rates of base-level change), and volumetric increments of erosion decreased over time (Bountry et al., 2018). The importance of floods in driving most of the post-dam removal reservoir sediment export, as observed in our study, contrasts with other previous dam removals where studies found little connection between post-dam-removal flow magnitude and the proportion or timing of sediment evacuated from the reservoir (Major et al., 2017). The independence between reservoir-sediment erosion and discharge magnitude found in previous studies has been attributed to the primacy of process-based erosion over event-based erosion, originally described in the conceptual model of Pizzuto (2002). In this conceptual model, process-based erosion (the 'process' being the disturbance caused by dam removal) is mostly independent of flow magnitude and reflects changes in reservoir equilibrium after dam removal (i.e. base-level fall, knickpoint retreat), whereas event-based changes are responses to later high flows (Pizzuto, 2002; Pearson et al., 2011). The importance of process-based erosion was illustrated during the removal of Marmot Dam on the Sandy River, Oregon (Major et al., 2012), removal of the two dams on the Elwha River, Washington (East et al., 2015), and in two eastern US dam removals described by Pearson et al. (2011) and Collins et al. (2017). In each of those cases, the major event driving geomorphic change was the removal of the dam itself and the subsequent base-level fall and reservoir-sediment export. In contrast, on the Carmel River the most notable geomorphic changes occurred in the second year following dam removal, during high flows. We attribute the different river response to dam removal on the Carmel River to two factors: (1) the Carmel having a relatively small base-level drop and relatively small subsequent increase in sediment supply following dam removal, due to sequestration of most

reservoir sediment; and (2) the Carmel River floods having been proportionally much larger, and earlier in the dam-removal response time frame, than those experienced on prior large dam removals.

The large, rare flows of 2017 exerted important controls over the newly developing channel planform in the former reservoir. Existing conceptual models of reservoir-sediment erosion and channel evolution identify a series of processes that typically occur in response to dam removal. These include reservoir drawdown and permanent base-level lowering, which induce knickpoint retreat through the reservoir sediment as well as channel incision and widening (Doyle *et al.*, 2002; Pizzuto, 2002; Cannatelli and Curran, 2012). Knickpoint migration, incision, and widening start at the dam site and propagate upstream. Although these general processes are common among various dam removals, the rates and details of channel evolution depend upon the rate of reservoir drawdown and the grain size and cohesive properties of the impounded sediment (Wilcox *et al.*, 2014; Randle *et al.*, 2015; Major *et al.*, 2017). On the Carmel River, we observed knickpoint retreat and channel widening in parts of the reservoir (Figure 6b), particularly in 2015 and 2016, but these changes were superseded in magnitude by new channel avulsion through the floodplain and widening of the active channel during floods in 2017 (Figure 4). Thus, the evolution of the San Clemente reservoir sediment deposit on the Carmel River differed fundamentally from reservoir evolution in previous dam removals. Instead of the expectation that geomorphic evolution is driven from downstream to upstream due to base-level fall (Doyle *et al.*, 2002, 2003), on the Carmel the most substantial geomorphic evolution (new channel avulsion and widening) originated from the upstream end of the former reservoir and propagated downstream, due to the influence of high flows. The channel configuration and evacuated sediment volume are therefore a result of superimposed downstream-driven and upstream-driven geomorphic forcing, a situation not evident in any prior large dam removal. The bed and bank sediments in the reservoir reach continue to be unstable, and this part of the former reservoir will remain a net sediment source until the channel morphology adjusts to a new equilibrium.

In the turbidity records, each flood in 2017 produced clockwise hysteresis loops (Figure 3). This indicates that despite large sediment exports from the river system and especially the former reservoir, the river remains in a state of sediment-supply limitation. In contrast, other turbidity records from the same floods on the central California coast on a watershed 65 km to the north show counterclockwise hysteresis (Conaway *et al.*, 2013; East *et al.*, 2018), reflecting arrival of substantial sediment from the upper watershed late in the flood hydrograph. Our turbidity data from the Carmel River do not show this (Figure 3). Although differences in sediment supply from tributaries (a function of lithology or gradient) may have affected the hysteresis pattern in our turbidity data, we consider this most likely attributable to the continued trapping of upper-watershed sediment behind Los Padres Dam, 11 km upstream of the former San Clemente Dam site (Figure 1). The clockwise hysteresis indicates that even though a large dam has been removed, releasing new sediment fluxes from the upper watershed and former reservoir, natural watershed processes have not been fully restored as long as the large dam higher up in the watershed continues to impound sediment.

The dam-removal sediment migrated downstream as a sediment pulse (Figures 5b and 5c), as observed in previous field (Zunka *et al.*, 2015; Pace *et al.*, 2017), laboratory (Cui *et al.*, 2003a; Sklar *et al.*, 2009) and theoretical modeling studies (Cui *et al.*, 2003b; Cui and Parker, 2005). Introduced sediment pulses may either disperse, translate downstream as a discrete sediment wave, or some combination of translation and dispersion (Lisle *et al.*, 2001; Sklar *et al.*, 2009). On the Carmel, changes in sediment thickness displayed evidence of translation and dispersion (Figure 5), as the pulse migrated downstream filling in deep pools. The initial pulse developed in the first year following dam removal (Figure 5b). Erosion of the upstream end of the pulse near the former dam site and the downstream increase in sediment thickness suggest pulse translation, while the rapid advancement of the leading edge and resulting pulse elongation (to > 30 km in 2017) are more typical of a dispersive wave (Figure 5c). Pulse translation observed on the Carmel River likely reflects the fine-grained nature of the upstream reservoir material relative to the ambient bed and the small volume of sediment introduced in the first year following dam removal, which both favor pulse translation (Lisle *et al.*, 2001; Cui *et al.*, 2003a; Sklar *et al.*, 2009). Sediment pulse dispersion was likely driven by the series of peak flows in the second year following dam removal, as pulse dispersion is more common during flow discharges that greatly exceed the sediment transport capacity (Humphries *et al.*, 2012).

At the reach scale, downstream channel adjustment to increased sediment supply mainly involved a decrease in overall relief (Figure 5), through pool-filling (Figures 6 and 7), with minimal topographic change on riffles. Pool filling is commonly observed after dam removal (Bountry *et al.*, 2013; Zunka *et al.*, 2015) and field studies have found evidence of decreased relief and pool filling resulting from increased sediment supply (Lisle, 1982; Madej, 1999, 2001). Rates of pool recovery following sedimentation are not widely reported in the literature, though Wohl and Cenderelli (2000) tracked sediment deposition and erosion patterns through a sequence of pools following a reservoir sediment release. They observed initial sediment evacuation in upstream pools, followed by more gradual transport and erosion in downstream pools. Results from our study showed a similar progression of pool response to increased sediment supply, with upstream pools close to the former dam site showing complete recovery to the pre-dam removal bed state (Figure 7b), but only partial pool recovery further downstream during our period of monitoring (Figure 7d). Pool infilling with fine sediment extended over 25 km downstream from the former dam site. Full pool recovery in these more distal reaches will depend on the magnitude, duration and timing of future flushing flows.

Overall, bed sediment texture became finer after dam removal, which is common when an introduced sediment pulse has a range of grain sizes (Cui *et al.*, 2003a). A more typical downstream fining pattern has begun to evolve due to the partial restoration of the natural sediment supply. At the bedform scale, textural changes involved deposition of sand and fine gravel in pools and gravel storage in riffles. This pattern of sediment sorting, with coarse sediment on riffles and fine sediment in pools, is commonly observed in low-sinuosity, gravel-bedded rivers with riffle-pool sequences (Keller, 1971; Thompson and Hoffman, 2001).

The post-dam-removal geomorphic and sedimentary changes on the Carmel River lead to several ecological implications. Changes to the bed texture of riffles indicate a gradual improvement in the gravel fractions suitable for steelhead spawning in reaches near the former dam site (Figurss 9c and 9d). Prior to dam removal the highest-quality spawning substrate was located in the lowermost reaches (rkm 11.1 to 2.4; Figures 9a and 9b), which commonly dry up entirely during the warm summer months. The introduction of higher-quality spawning habitat in upstream reaches with perennial flow (rkm 28.4 to 13.1 in Figure 9d) should aid fish survival in early life-stages. Reduced pool depths could impact steelhead rearing habitat quality, if pools become too shallow for

young fish. Pools tend to become unuseable for rearing steelhead at water depths < 0.2 m for steelhead in their first year and < 0.4 m in subsequent years (Spina, 2000, 2003). Pools < 0.4 m deep were not widely observed during our study. Typical timescales for river channels to return to pre-dam removal bed states have tended to occur over a few years (Pearson *et al.*, 2011), though full pool recovery on the Carmel could take longer due to the episodic nature of the flow regime in this Mediterranean hydroclimate.

Conclusions

The removal of San Clemente Dam on the Carmel River represents the largest dam removal to date in a Mediterranean hydroclimatic setting, and illustrates how physiographic setting can influence the river response to dam removal. Channel change and habitat development in Mediterranean rivers are highly sensitive to the punctuated delivery of water and sediment (Kondolf *et al.*, 2013). As such, and in contrast to dam removals in other bioregions, we found that flood events were essential in driving the response of the channel to dam removal. The small degree of base-level lowering during removal of San Clemente Dam likely enhanced the importance of post-dam-removal floods; dam removals in other Mediterranean rivers with larger base-level drops could potentially experience more rapid reservoir-sediment erosion earlier in the dam-removal-response time frame. Nevertheless, the role of floods in driving geomorphic changes is likely to be highly important in other semi-arid river systems with variable flow and sediment regimes where dam removal is being considered or planned.

Our field measurements provided novel insights on the coupled reservoir–river system response to dam removal and subsequent high flows. Initial knickpoint development, channel widening and avulsion in the old reservoir sediments generated sediment transport to reaches downstream of the former dam site. The avulsion of a new channel originating at the upstream end of the former reservoir in response to large floods was unique to this study, as no other analogous geomorphic response in a reservoir deposit has been reported in previous dam-removal studies. In the two years since the removal of San Clemente Dam, a sediment pulse moved more than ~30 km (to the river mouth), exhibiting a combination of pulse dispersion and translation, with maximum travel distances delayed until large floods in the second year. Reach-scale morphology responded to increased sediment supply primarily by pool-filling and decreased cross-sectional relief. The riverbed grain size generally fined in reaches below the dam site.

The restoration of natural processes via dam removal are often anticipated to benefit the river ecosystem, but overall ecosystem response to increased sediment supply entails considerable uncertainty. Positive impacts observed in the Carmel River included modest increases and greater spatial distribution of salmonid-spawning substrate below the dam. The initial physical response reduced pool depths, which could have seasonal and local impacts to specific life stages of steelhead. Given the dependence of river response to strong seasonal flow variation in this hydroclimatic setting, the realization of long-term ecological benefits in Mediterranean rivers such as the Carmel River will likely be more reliant on infrequent channel-shaping floods than in other bioregions.

Acknowledgements—August Delforge, Sheldon Leiker, John Silveus, Elizabeth Geisler, Justin Bolger, Alejandra Reyes and Zane Mortensen helped collect field data. The authors thank Mathias Collins for valuable feedback on an earlier draft. The manuscript greatly benefitted from the thorough and constructive reviews provided by Christian Braudrick and an anonymous reviewer. All river-channel topography, grain-size and turbidity data used in this study are available through the US Geological Survey Data Release, https://doi.org/10.5066/F74M93HF.

References

Allen MB, Engle RO, Zendt JS, Shrier FC, Wilson JT, Connolly PJ. 2016. Salmon and Steelhead in the White Salmon River after the removal of condit dam-planning efforts and recolonization results. *Fisheries* **41**: 190–203. https://doi.org/10.1080/03632415.2016.1150839.

Andrews ED, Antweiler RC. 2012. Sediment fluxes from California coastal rivers: the influences of climate, geology, and topography. *Journal of Geology* **120**: 349–366. https://doi.org/10.1086/665733.

Bao JW, Michelson SA, Neiman PJ, Ralph FM, Wilczak JM. 2006. Interpretation of enhanced integrated water vapor bands associated with extratropical cyclones: their formation and connection to tropical moisture. *Monthly Weather Review* **134**: 1063–1080. https://doi.org/10.1175/Mwr3123.1.

Bednarek AT. 2001. Undamming rivers: a review of the ecological impacts of dam removal. *Environmental Management* **27**: 803–814. https://doi.org/10.1007/s002670010189.

Bellmore RJ, Duda JJ, Craig LS, Greene SL, Torgersen CE, Collins MJ, Vittum K. 2017. Status and trends of dam removal research in the United States. *Wiley Interdisciplinary Reviews Water* **4**. https://doi.org/10.1002/wat2.e1164.

Boughton DA, East AE, Hampson L, Kiernan JD, Leiker S, Mantua N, Nicol C, Smith D, Urquhart K, Williams TH, Harrison LR. 2016. *Removing a Dam and Re-routing a River: Will Expected Benefits for Stelhead be Realized in Carmel River, California?* NOAA Technical Memorandum NMFS, NOAA-TM-NMFS-SWFSC-553.89. National Oceanic and Atmospheric Administration: Silver Spring, MD. DOI: https://doi.org/10.7289/V5/TM-SWFSC-553.

Bountry J, Randle TJ, Ritchie A. 2018. *Adaptive Sediment Management Program Final Report for the Elwha River Restoration Project*. US Department of the Interior, Bureau of Reclamation, US Geological Survey, National Park Service: Reston, VA 276.

Bountry JA, Lai YG, Randle TJ. 2013. Sediment impacts from the Savage Rapids Dam removal, Rogue River, Oregon. In *The Challenges of Dam Removal and River Restoration*, Graff JVD, Evans JE (eds). Boulder, CO.: Geological Society of America.

Brasington J, Vericat D, Rychkov I. 2012. Modeling river bed morphology, roughness, and surface sedimentology using high resolution terrestrial laser scanning. *Water Resources Research* **48**. https://doi.org/10.1029/2012wr012223.W11519.

Cannatelli KM, Curran JC. 2012. Importance of hydrology on channel evolution following dam removal: case study and conceptual model. *Journal of Hydraulic Engineering* **138**: 377–390. https://doi.org/10.1061/(ASCE)HY.1943-7900.0000526.

Cayan DR, Redmond KT, Riddle LG. 1999. ENSO and hydrologic extremes in the western United States. *Journal of Climate* **12**: 2881–2893. https://doi.org/10.1175/1520-0442(1999)012<2881:Eaheit>2.0.Co;2.

Claeson SM, Coffin B. 2016. Physical and biological responses to an alternative removal strategy of a moderate-sized dam in Washington, USA. *River Research and Applications* **32**: 1143–1152. https://doi.org/10.1002/rra.2935.

Collins MJ, Snyder NP, Boardman G, Banks WSL, Andrews M, Baker ME, Conlon M, Gellis A, McClain S, Miller A, Wilcock P. 2017. Channel response to sediment release: insights from a paired analysis of dam removal. *Earth Surface Processes and Landforms* **42**: 1636–1651. https://doi.org/10.1002/esp.4108.

Conaway CH, Draut AE, Echols KR, Storlazzi CD, Ritchie A. 2013. Episodic suspended sediment transport and elevated polycyclic aromatic hydrocarbon concentrations in a small, mountainous river in coastal California. *River Research and Applications* **29**: 919–932. https://doi.org/10.1002/rra.2582.

Cui YT, Parker G. 2005. Numerical model of sediment pulses and sediment-supply disturbances in mountain rivers. *Journal of Hydraulic Engineering ASCE* **131**: 646–656. https://doi.org/10.1061/(Asce)0733-9429(2005)131:8(646).

Cui YT, Parker G, Lisle TE, Gott J, Hansler-Ball ME, Pizzuto JE, Allmendinger NE, Reed JM. 2003a. Sediment pulses in mountain rivers: 1. Experiments. *Water Resources Research* **39**(9): 1239. https://doi.org/10.1029/2002wr001803.

Cui YT, Parker G, Pizzuto J, Lisle TE. 2003b. Sediment pulses in mountain rivers: 2. Comparison between experiments and numerical predictions. *Water Resources Research* **39**(9): 1240. https://doi.org/10.1029/2002wr001805.

Dettinger M. 2011. Climate change, atmospheric rivers, and floods in california – a multimodel analysis of storm frequency and magnitude changes. *Journal of the American Water Resources Association* **47**: 514–523. https://doi.org/10.1111/j.1752-1688.2011.00546.x.

Dettman DD, Hanna BM. 1991. *Development of a Substrate Suitability Curve for Adult Steelhead Spawning Habitat in the Carmel River Downstream of San Clement Dam*, Tech Memo 91-4. Monterey Peninsula Water Management District: Monterey, CA; 22.

Doyle MW, Stanley EH, Harbor JM. 2002. Geomorphic analogies for assessing probable channel response to dam removal. *Journal of the American Water Resources Association* **38**: 1567–1579. https://doi.org/10.1111/j.1752-1688.2002.tb04365.x.

Doyle MW, Stanley EH, Harbor JM. 2003. Channel adjustments following two dam removals in Wisconsin. *Water Resources Research* **39**: 1011. https://doi.org/10.1029/2002wr001714.

Doyle MW, Stanley EH, Havlick DG, Kaiser MJ, Steinbach G, Graf WL, Galloway GE, Riggsbee JA. 2008. Environmental science – aging infrastructure and ecosystem restoration. *Science* **319**: 286–287. https://doi.org/10.1126/science.1149852.

East AE, Pess GR, Bountry JA, Magirl CS, Ritchie AC, Logan JB, Randle TJ, Mastin MC, Minear JT, Duda JJ, Liermann MC, McHenry ML, Beechie TJ, Shafroth PB. 2015. Large-scale dam removal on the Elwha River, Washington, USA: river channel and floodplain geomorphic change. *Geomorphology* **228**: 765–786. https://doi.org/10.1016/j.geomorph.2014.08.028.

East AE, Stevens AW, Ritchie AC, Barnard PL, Campbell-Swarzenski P, Collins BD, Conaway CH. 2018. A regime shift in sediment export from a coastal watershed during a record wet winter, California: implications for landscape response to hydroclimatic extremes. *Earth Surface Processes and Landforms*. https://doi.org/10.1002/esp.4415.

Evans E, Wilcox AC. 2014. Fine sediment infiltration dynamics in a gravel-bed river following a sediment pulse. *River Research and Applications* **30**: 372–384. https://doi.org/10.1002/rra.2647.

Foley MM, Bellmore JR, O'Connor JE, Duda JJ, East AE, Grant GE, Anderson CW, Bountry JA, Collins MJ, Connolly PJ, Craig LS, Evans JE, Greene SL, Magilligan FJ, Magirl CS, Major JJ, Pess GR, Randle TJ, Shafroth PB, Torgersen CE, Tullos D, Wilcox AC. 2017a. Dam removal: listening in. *Water Resources Research* **53**(7): 5229–5246.

Foley MM, Magilligan FJ, Torgersen CE, Major JJ, Anderson CW, Connolly PJ, Wieferich D, Shafroth PB, Evans JE, Infante D, Craig LS. 2017b. Landscape context and the biophysical response of rivers to dam removal in the United States. *PLoS One* **12**(7): e0180107. https://doi.org/10.1371/journal.pone.0180107.

Galay VJ. 1983. Causes of river bed degradation. *Water Resources Research* **19**: 1057–1090. https://doi.org/10.1029/WR019i005p01057.

Gilbert GK. 1917. *Hydraulic-mining Debris in the Sierra Nevada*. US Geological Survey: Reston, VA 188.

Grant GE, Lewis SL. 2015. The remains of the dam: what have we learned from 15 years of U.S. dam removals? In *Engineering Geology for Society and Territory*, Lollino G, Arattano M, Rinaldi M, Giustolisi O, Marechal J-C, Grant GE (eds). Springer International Publishing Cham: Switzerland; 31–35.

Grant GE, Schmidt JC, Lewis SL. 2003. A geological framework for interpreting downstream effects of dams on rivers. *Water Science and Application* **7**: 209–225.

Gray AB, Pasternack GB, Watson EB, Warrick JA, Goni MA. 2015. The effect of El Nino Southern Oscillation cycles on the decadal scale suspended sediment behavior of a coastal dry-summer subtropical catchment. *Earth Surface Processes and Landforms* **40**: 272–284. https://doi.org/10.1002/esp.3627.

Guthrie RH, Friele P, Allstadt K, Roberts N, Evans SG, Delaney KB, Roche D, Clague JJ, Jakob M. 2012. The 6 August 2010 Mount Meager rock slide-debris flow, Coast Mountains, British Columbia: characteristics, dynamics, and implications for hazard and risk assessment. *Natural Hazards and Earth System Sciences* **12**: 1277–1294. https://doi.org/10.5194/nhess-12-1277-2012.

Guy HP. 1969. Laboratory theory and methods for sediment analysis. In *U.S. Geological Survey Techniques of Water-Resources Investigations, book 5, chapter C1*. US Geological Survey: Reston, VA 58.

Humphries R, Venditti JG, Sklar LS, Wooster JK. 2012. Experimental evidence for the effect of hydrographs on sediment pulse dynamics in gravel-bedded rivers. *Water Resources Research* **48**. https://doi.org/10.1029/2011wr010419.

Ibisate A, Ollero A, Ballarin D, Horacio J, Mora D, Mesanza A, Ferrer-Boix C, Acin V, Granado D, Martin-Vide JP. 2016. Geomorphic monitoring and response to two dam removals: rivers Urumea and Leitzaran (Basque Country, Spain). *Earth Surface Processes and Landforms* **41**: 2239–2255. https://doi.org/10.1002/esp.4023.

Keller EA. 1971. Areal sorting of bed-load material – hypothesis of velocity reversal. *Geological Society of America Bulletin* **82**: 753–756.

Klein M. 1984. Anti clockwise hysteresis in suspended sediment concentration during individual storms – Holbeck Catchment – Yorkshire, England. *Catena* **11**: 251–257. https://doi.org/10.1016/S0341-8162(84)80024-7.

Kondolf GM, Gao Y, Annandale GW, Morris GL, Jiang E, Zhang J, Cao Y, Carling P, Fu K, Guo Q, Hotchkiss R, Peteuil C, Sumi T, Wang H, Wang Z, Wei Z, Wu B, Wu C, Yang CH. 2014. Sustainable sediment management in reservoirs and regulated rivers: experiences from five continents. *Earth's Future* **2**: 256–280. https://doi.org/10.1002/2013EF000184.

Kondolf GM, Podolak K, Grantham T. 2013. Restoring mediterranean-climate rivers. *Hydrobiologia* **719**: 527–545. https://doi.org/10.1007/s10750-012-1363-y.

Kondolf GM, Wolman MG. 1993. The sizes of salmonid spawning gravels. *Water Resources Research* **29**: 2275–2285.

Lane SN, Westaway RM, Murray Hicks D. 2003. Estimation of erosion and deposition volumes in a large, gravel-bed, braided river using synoptic remote sensing. *Earth Surface Processes and Landforms* **28**: 249–271. https://doi.org/10.1002/esp.483.

Lauer JW, Parker G. 2008. Net local removal of floodplain sediment by river meander migration. *Geomorphology* **96**: 123–149. https://doi.org/10.1016/j.geomorph.2007.08.003.

Lisle TE. 1982. Effects of aggradation and degradation on riffle-pool morphology in natural gravel channels, northwestern California. *Water Resources Research* **18**: 1643–1651. https://doi.org/10.1029/WR018i006p01643.

Lisle TE, Cui YT, Parker G, Pizzuto JE, Dodd AM. 2001. The dominance of dispersion in the evolution of bed material waves in gravel-bed rivers. *Earth Surface Processes and Landforms* **26**: 1409–1420. https://doi.org/10.1002/esp.300.

Madej MA. 1999. Temporal and spatial variability in thalweg profiles of a gravel-bed river. *Earth Surface Processes and Landforms* **24**: 1153–1169.

Madej MA. 2001. Development of channel organization and roughness following sediment pulses in single-thread, gravel bed rivers. *Water Resources Research* **37**: 2259–2272. https://doi.org/10.1029/2001wr000229.

Magilligan FJ, Graber BE, Nislow KH, Chipman JW, Sneddon CS, Fox CA. 2016. River restoration by dam removal: enhancing connectivity at watershed scales. *Elementa: Science of the Anthropocene* **4**. https://doi.org/10.12952/journal.elementa.000108.

Major JJ, East AE, O'Connor JE, Grant GE, Wilcox AC, Magirl CS, Collins MJ, Tullos DD. 2017. Geomorphic responses to dam removal in the United States – a two-decade perspective. In *Gravel-Bed Rivers*. John Wiley & Sons: Chichester; 355–383.

Major JJ, O'Connor JE, Podolak CJ, Keith MK, Grant GE, Spicer KR, Pittman S, Bragg HM, Wallick JR, Tanner DQ, Rhode A, Wilcock PR. 2012. *Geomorphic Response of the Sandy River, Oregon, to Removal of Marmot Dam*. US Geological Survey: Reston, VA 64.

MEI. 2005. *Hydraulic and Sediment-transport Analysis of the Carmel River Bypass Option, California*. Prepared by Mussetter Engineering Inc. for California American Water: Fort Collins, CO 74.

Pace KM, Tullos D, Walter C, Lancaster S, Segura C. 2017. Sediment pulse behaviour following dam removal in gravel-bed rivers. *River Research and Applications* **33**: 102–112. https://doi.org/10.1002/rra.3064.

Pearson AJ, Snyder NP, Collins MJ. 2011. Rates and processes of channel response to dam removal with a sand-filled impoundment. *Water Resources Research* **47**: W08504. https://doi.org/10.1029/2010wr009733.

Pess GR, Quinn TP, Gephard SR, Saunders R. 2014. Re-colonization of Atlantic and Pacific rivers by anadromous fishes: linkages between life history and the benefits of barrier removal. *Reviews in Fish Biology and Fisheries* **24**: 881–900. https://doi.org/10.1007/s11160-013-9339-1.

Pierson TC, Major JJ. 2014. Hydrogeomorphic effects of explosive volcanic eruptions on drainage basins. *Annual Review of Earth and Planetary Sciences* **42**: 469–507. https://doi.org/10.1146/annurev-earth-060313-054913.

Pizzuto J. 2002. Effects of dam removal on river form and process. *Bioscience* **52**: 683–691. https://doi.org/10.1641/0006-3568(2002)052[0683:Eodror]2.0.Co;2.

Pizzuto J, O'Neal M. 2009. Increased mid-twentieth century riverbank erosion rates related to the demise of mill dams, South River, Virginia. *Geology* **37**: 19–22. DOI: https://doi.org/10.1130/G25207a.1

Poff NL, Hart DD. 2002. How dams vary and why it matters for the emerging science of dam removal. *Bioscience* **52**: 659–668.

Quinn T, Bond M, Brenkman S, Paradis R, Peters R. 2017. Re-awakening dormant life history variation: stable isotopes indicate anadromy in bull trout following dam removal on the Elwha River, Washington. *Environmental Biology of Fishes* **100**: 1659–1671.

Randle TJ, Bounty JA, Ritchie A, Wille K. 2015. Large-scale dam removal on the Elwha River, Washington, USA: erosion of reservoir sediment. *Geomorphology* **246**: 709–728. https://doi.org/10.1016/j.geomorph.2014.12.045.

Rasmussen PP, Gray JR, Glysson GD, Ziegler AC. 2009. Guidelines and procedures for computing time-series suspended-sediment concentrations and loads from in-stream turbidity-sensor and streamflow data. In *U.S. Geological Survey Techniques and Methods, book 3, chapter C4*. US Geological Survey: Reston, VA 53.

Reusser L, Bierman P, Rood D. 2015. Quantifying human impacts on rates of erosion and sediment transport at a landscape scale. *Geology* **43**: 171–174. https://doi.org/10.1130/G36272.1.

Rollet AJ, Piegay H, Dufour S, Bornette G, Persat H. 2014. Assessment of consequences of sediment deficit on a gravel river bed downstream of dams in restoration perspectives: application of a multicriteria, hierarchical and spatially explicit diagnosis. *River Research and Applications* **30**: 939–953. https://doi.org/10.1002/rra.2689.

Schmidt JC, Wilcock PR. 2008. Metrics for assessing the downstream effects of dams. *Water Resources Research* **44**: W04404. https://doi.org/10.1029/2006wr005092.

Sklar LS, Fadde J, Venditti JG, Nelson P, Wydzga MA, Cui YT, Dietrich WE. 2009. Translation and dispersion of sediment pulses in flume experiments simulating gravel augmentation below dams. *Water Resources Research* **45**: W08439. https://doi.org/10.1029/2008wr007346.

Smith D, Newman W, Watson F, Hameister J. 2004. *Physical and hydrologic assessment of Carmel River watershed, California: Central Coast Watershed Studies*, Report no. WI-2004-05/2. California State University Monterey Bay: Monterey, CA 94.

Spina AP. 2000. Habitat partitioning in a patchy environment: considering the role of intraspecific competition. *Environmental Biology of Fishes* **57**: 393–400.

Spina AP. 2003. Habitat associations of steelhead trout near the southern extent of their range. *California Fish & Game* **89**: 81–95.

Syvitski JPM, Vorosmarty CJ, Kettner AJ, Green P. 2005. Impact of humans on the flux of terrestrial sediment to the global coastal ocean. *Science* **308**: 376–380. https://doi.org/10.1126/science.1109454.

Thompson DM, Hoffman KS. 2001. Equilibrium pool dimensions and sediment-sorting patterns in coarse-grained, New England channels. *Geomorphology* **38**: 301–316. https://doi.org/10.1016/S0169-555x(00)00100-8.

Tonra CM, Sager-Fradkin K, Morley SA, Duda JJ, Marra PP. 2015. The rapid return of marine-derived nutrients to a freshwater food web following dam removal. *Biological Conservation* **192**: 130–134. https://doi.org/10.1016/j.biocon.2015.09.009.

Topping DJ, Rubin DM, Melis TS. 2007. Coupled changes in sand grain size and sand transport driven by changes in the upstream supply of sand in the Colorado River: relative importance of changes in bed-sand grain size and bed-sand area. *Sedimentary Geology* **202**: 538–561. https://doi.org/10.1016/j.sedgeo.2007.03.016.

Topping DJ, Rubin DM, Vierra LE. 2000. Colorado River sediment transport – 1. Natural sediment supply limitation and the influence of Glen Canyon Dam. *Water Resources Research* **36**: 515–542. https://doi.org/10.1029/1999wr900285.

Tullos DD, Finn DS, Walter C. 2014. Geomorphic and ecological disturbance and recovery from two small dams and their removal. *PLoS One* **9**(9): e108091. https://doi.org/10.1371/journal.pone.0108091.

Wang HW, Kuo WC. 2016. Geomorphic responses to a large check-dam removal on a mountain river in Taiwan. *River Research and Applications* **32**: 1094–1105. https://doi.org/10.1002/rra.2929.

Ward JV, Stanford JA. 1995. Ecological connectivity in alluvial river ecosystems and its disruption by flow regulation. *Regulated Rivers: Research & Management* **11**: 105–119. https://doi.org/10.1002/rrr.3450110109.

Warrick JA, Bountry JA, East AE, Magirl CS, Randle TJ, Gelfenbaum G, Ritchie AC, Pess GR, Leung V, Duda JJ. 2015. Large-scale dam removal on the Elwha River, Washington, USA: source-to-sink sediment budget and synthesis. *Geomorphology* **246**: 729–750. https://doi.org/10.1016/j.geomorph.2015.01.010.

Wheaton JM, Brasington J, Darby SE, Sear DA. 2010. Accounting for uncertainty in DEMs from repeat topographic surveys: improved sediment budgets. *Earth Surface Processes and Landforms* **35**: 136–156. https://doi.org/10.1002/esp.1886.

Wilcox AC, O'Connor JE, Major JJ. 2014. Rapid reservoir erosion, hyperconcentrated flow, and downstream deposition triggered by breaching of 38 m tall Condit Dam, White Salmon River, Washington. *Journal of Geophysical Research - Earth Surface* **119**: 1376–1394.

Wildman LAS, MacBroom JG. 2005. The evolution of gravel bed channels after dam removal: case study of the Anaconda and Union City Dam removals. *Geomorphology* **71**: 245–262. https://doi.org/10.1016/j.geomorph.2004.08.018.

Wohl EE, Cenderelli DA. 2000. Sediment deposition and transport patterns following a reservoir sediment release. *Water Resources Research* **36**: 319–333. https://doi.org/10.1029/1999wr900272.

Wolman MG. 1954. A method of sampling coarse river-bed material. *American Geophysical Union* **35**: 951–956.

Yang XK, Lu XX. 2014. Estimate of cumulative sediment trapping by multiple reservoirs in large river basins: an example of the Yangtze River basin. *Geomorphology* **227**: 49–59. https://doi.org/10.1016/j.geomorph.2014.01.014.

Zunka JPP, Tullos DD, Lancaster ST. 2015. Effects of sediment pulses on bed relief in bar-pool channels. *Earth Surface Processes and Landforms* **40**: 1017–1028. https://doi.org/10.1002/esp.3697.